

# Synthesis, structural studies and catalytic activity of dioxidomolybdenum(VI) complexes with aroylhydrazones of naphthol-derivative



Sagarika Pasayat<sup>a</sup>, Subhashree P. Dash<sup>a</sup>, Satabdi Roy<sup>a</sup>, Rupam Dinda<sup>a,\*</sup>, Sarita Dhaka<sup>b</sup>, Mannar R. Maurya<sup>b</sup>, Werner Kaminsky<sup>c</sup>, Yogesh P. Patil<sup>d</sup>, M. Nethaji<sup>d</sup>

<sup>a</sup> Department of Chemistry, National Institute of Technology, Rourkela 769008, Odisha, India

<sup>b</sup> Department of Chemistry, Indian Institute of Technology Roorkee, Roorkee 247667, India

<sup>c</sup> Department of Chemistry, University of Washington, Box 351700, Seattle, WA 98195, USA

<sup>d</sup> Department of Inorganic and Physical Chemistry, Indian Institute of Science, Bangalore 560012, India

## ARTICLE INFO

### Article history:

Received 20 May 2013

Accepted 22 August 2013

Available online 3 September 2013

### Keywords:

Aroylhydrazones

Naphthol-derivative

Dioxidomolybdenum(VI) complexes

X-ray crystal structure

Catalytic oxidation of benzoin

Oxidative bromination

## ABSTRACT

Reaction of the salicylhydrazone of 2-hydroxy-1-naphthaldehyde ( $H_2L^1$ ), anthranilylhydrazone of 2-hydroxy-1-naphthaldehyde ( $H_2L^2$ ), benzoylhydrazone of 2-hydroxy-1-acetonaphthone ( $H_2L^3$ ) and anthranilylhydrazone of 2-hydroxy-1-acetonaphthone ( $H_2L^4$ ; general abbreviation  $H_2L$ ) with  $[MoO_2(-acac)_2]$  afforded a series of 5- and 6- coordinate Mo(VI) complexes of the type  $[MoO_2L^{1-2}(ROH)]$  [where  $R = C_2H_5$  (**1**) and  $CH_3$  (**2**)], and  $[MoO_2L^{3-4}]$  (**3** and **4**). The substrate binding capacity of **1** has been demonstrated by the formation of one mononuclear mixed-ligand dioxidomolybdenum complex  $[MoO_2L^1(Q)]$  {where  $Q = \gamma$ -picoline (**1a**)}. Molecular structure of all the complexes (**1**, **1a**, **2**, **3** and **4**) is determined by X-ray crystallography, demonstrating the dibasic tridentate behavior of ligands. All the complexes show two irreversible reductive responses within the potential window  $-0.73$  to  $-1.08$  V, due to  $Mo^{VI}/Mo^V$  and  $Mo^V/Mo^{IV}$  processes. Catalytic potential of these complexes was tested for the oxidation of benzoin using 30% aqueous  $H_2O_2$  as an oxidant in methanol. At least four reaction products, benzoic acid, benzaldehyde, dimethylacetone, methyl benzoate and benzil were obtained with the 95–99% conversion under optimized reaction conditions. Oxidative bromination of salicylaldehyde, a functional mimic of haloperoxidases, in aqueous  $H_2O_2/KBr$  in the presence of  $HClO_4$  at room temperature has also been carried out successfully.

© 2013 Elsevier Ltd. All rights reserved.

## 1. Introduction

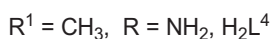
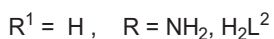
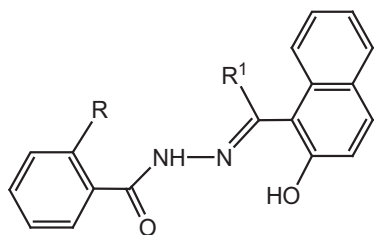
Schiff bases, characterized by the azomethine group ( $-RC=N-$ ), form a significant class of compounds in medicinal and pharmaceutical chemistry and are known to have biological applications due to their antibacterial [1–6], antifungal [3–6] and antitumor [7,8] activity. The incorporation of transition metals into these compounds leads to the enhancement of their biological activities and decrease in the cytotoxicity of both the metal ion and Schiff base ligand [9–11]. On the other hand, aroylhydrazones are excellent multidentate ligands for transition metals. They have been shown to exhibit a range of biological e.g. anti-moebic activity [12] and DNA synthesis inhibition or antiproliferative behavior [13–15]. For quite some time, we have been engaged in a program aimed at credible synthesis of oxygen and nitrogen co-ordinated transition metal compounds in order to approach the biological co-ordination units as potential lead molecules for drug designing.

Accordingly, we have synthesized and examined a number of transition metal-Schiff base compounds using aroylhydrazone as tridentate (ONO) – donor ligand [16–18]. Their properties can be tuned by modification of either the aromatic aldehyde or the hydrazide component. Our aim was to increase lipophilicity using bulky aromatic groups and to investigate the influence on the coordination sphere as well as reactivity by the use of aroylhydrazone of naphthol-derivatives.

The coordination chemistry of molybdenum has become a fascinating area of research in recent years because of the presence of molybdenum in metalloenzymes [19–25]. Catalytic applications of molybdenum complexes in organic transformations, particularly in the epoxidation of alkenes have been explored much as evidenced by number of publications [26–39]. The catalytic activity of molybdenum complexes are sensitive to the donor/acceptor ability of the ligand, and to steric and strain factors. Therefore, we have designed sterically hindered/bulky ONO donor aroylhydrazones of naphthol-derivative (Scheme 1) in the light of above factors to prepare dioxidomolybdenum(VI) complexes. Varying the steric bulk of the aroylhydrazone ligands also controls the

\* Corresponding author. Tel.: +91 661 246 2657; fax: +91 661 246 2022.

E-mail address: [rupamdinda@nitrrkl.ac.in](mailto:rupamdinda@nitrrkl.ac.in) (R. Dinda).



**Scheme 1.** Schematic representation of Ligand.

coordination number of the molybdenum in these complexes. Novel structural features, reactivity patterns of these complexes and their catalytic activity for the oxidation of benzoin are reported here. Selective transformation of  $\alpha$ -hydroxyketone to the corresponding  $\alpha$ -diketone is one of the most important fundamental reactions in organic chemistry [40,41]. The catalytic potential of dioxidomolybdenum(VI) complexes for the oxidative bromination of salicylaldehyde, as functional mimic of haloperoxidase has also been explored.

## 2. Experimental

### 2.1. Materials

[MoO<sub>2</sub>(acac)<sub>2</sub>] was prepared as described in the literature [42]. Reagent grade solvents were dried and distilled prior to use. All other chemicals were reagent grade, available commercially and used as received. Commercially available TBAP (tetra butyl ammonium perchlorate) was dried and used as a supporting electrolyte for recording cyclic voltammograms of the complexes.

### 2.2. Physical measurements

Elemental analyses were performed on a Vario ELcube CHNS Elemental analyzer. IR spectra were recorded on a Perkin-Elmer Spectrum RXI spectrometer. <sup>1</sup>H NMR spectra were recorded with a Bruker Ultra shield 400 MHz spectrometer using SiMe<sub>4</sub> as an internal standard. Electronic spectra were recorded on a Lambda25, PerkinElmer spectrophotometer. Electrochemical data were collected using a PAR electrochemical analyzer and a PC-controlled Potentiostat/Galvanostat (PAR 273A) at 298 K in a dry nitrogen atmosphere. Cyclic voltammetry experiments were carried out with a platinum working electrode, platinum auxiliary electrode, Ag/AgCl as reference electrode and TBAP as supporting electrolyte. A Shimadzu 2010 plus gas-chromatograph fitted with an Rtx-1 capillary column (30 m × 0.25 mm × 0.25 μm) and a FID detector was used to analyze the reaction products and their quantifications were made on the basis of the relative peak area of the respective product. The identity of the products was confirmed using a GC-MS model Perkin-Elmer, Clarus 500 and comparing the fragments of each product with the library available. The percent conversion of substrate and selectivity of products was calculated from GC data using the formulae:

%Conversion of substrate = 100

$$= \frac{\text{Peak area of a substrate}}{\text{Total area of substrate + products}} \times 100$$

%Selectivity of a product =  $\frac{\text{Peak area of a product}}{\text{Total area of products}} \times 100$

### 2.3. Synthesis of Ligands (H<sub>2</sub>L<sup>1-4</sup>)

Schiff base ligands, H<sub>2</sub>L<sup>1-4</sup> were prepared by the condensation of carbonyl compounds and the respective acidhydrazide in equimolar ratio in ethanol medium by a standard procedure [43]. The resulting yellowish- white compounds were filtered, washed with ethanol and dried over fused CaCl<sub>2</sub>.

**H<sub>2</sub>L<sup>1</sup>:** Yield: 0.22 g (72%). *Anal. Calc.* for C<sub>18</sub>H<sub>14</sub>N<sub>2</sub>O<sub>3</sub>: C, 70.58; H, 4.57; N, 9.15. Found: C, 70.59; H, 4.54; N, 9.12%. <sup>1</sup>H NMR (DMSO-d<sub>6</sub>, 400 MHz) δ; 12.74 (s, 1H, naphthyl-OH), 12.07 (s, 1H, NH), 11.87 (s, 1H, aryl-OH), 9.54 (s, 1H, HC=N), 8.33–6.62 (m, 10H, Aromatic) ppm. <sup>13</sup>C NMR (DMSO-d<sub>6</sub>, 100 MHz) δ; 163.72, 158.51, 157.89, 147.44, 133.78, 132.68, 131.44, 128.69, 128.55, 127.57, 127.50, 123.33, 120.73, 118.92, 118.65, 117.05, 115.48, 108.36.

**H<sub>2</sub>L<sup>2</sup>:** Yield: 0.19 g (62%). *Anal. Calc.* for C<sub>18</sub>H<sub>15</sub>N<sub>3</sub>O<sub>2</sub>: C, 70.81; H, 4.90; N, 13.77. Found: C, 70.78; H, 4.92; N, 13.75%. <sup>1</sup>H NMR (DMSO-d<sub>6</sub>, 400 MHz) δ; 12.97 (s, 1H, naphthyl-OH), 12.04 (s, 1H, NH), 9.47 (s, 1H, HC=N), 8.18–6.64 (m, 10H, Aromatic), 6.61 (s, 2H, NH<sub>2</sub>) ppm. <sup>13</sup>C NMR (DMSO-d<sub>6</sub>, 100 MHz) δ; 165.12, 158.33, 150.93, 146.33, 133.18, 132.91, 132.07, 129.45, 128.57, 128.25, 128.16, 123.96, 120.88, 119.42, 117.12, 115.14, 112.62, 109.06.

**H<sub>2</sub>L<sup>3</sup>:** Yield: 0.18 g (60%). *Anal. Calc.* for C<sub>19</sub>H<sub>16</sub>N<sub>2</sub>O<sub>2</sub>: C, 74.89; H, 5.09; N, 9.10. Found: C, 74.90; H, 5.07; N, 9.11%. <sup>1</sup>H NMR (DMSO-d<sub>6</sub>, 400 MHz) δ; 10.31 (s, 1H, naphthyl-OH), 9.55 (s, 1H, NH), 7.91–7.27 (m, 11H, Aromatic), 2.34 (s, 3H, CH<sub>3</sub>) ppm. <sup>13</sup>C NMR (DMSO-d<sub>6</sub>, 100 MHz) δ; 153.71, 152.63, 134.24, 131.82, 131.51, 130.21, 129.06, 128.76, 128.36, 128.23, 127.86, 127.43, 126.99, 123.67, 123.19, 118.99, 118.71, 113.74, 24.30.

**H<sub>2</sub>L<sup>4</sup>:** Yield: 0.21 g (65%). *Anal. Calc.* for C<sub>19</sub>H<sub>17</sub>N<sub>3</sub>O<sub>2</sub>: C, 71.47; H, 5.32; N, 13.16. Found: C, 71.45; H, 5.33; N, 13.15%. <sup>1</sup>H NMR (DMSO-d<sub>6</sub>, 400 MHz) δ; 10.35 (s, 1H, naphthyl-OH), 9.17 (s, 1H, NH), 7.91–6.23 (m, 10H, Aromatic), 6.05 (s, 2H, NH<sub>2</sub>), 2.35 (s, 3H, CH<sub>3</sub>) ppm. <sup>13</sup>C NMR (DMSO-d<sub>6</sub>, 100 MHz) δ; 153.98, 152.47, 127.36, 149.84, 132.47, 131.56, 130.22, 129.09, 128.34, 127.98, 122.67, 123.78, 123.14, 118.94, 117.04, 115.46, 114.69, 113.59, 24.15.

### 2.4. Synthesis of complexes (1–4)

These complexes were prepared modifying a previously published procedure [44–46]. To a refluxing solution of ligand, H<sub>2</sub>L<sup>1-4</sup> (1.0 mmol) in 30 mL of alcohol {ethanol (**1** and **2**) and methanol (**3** and **4**)}, 1.0 mmol of MoO<sub>2</sub>(acac)<sub>2</sub> was added. The color of the solution changed to dark red. The mixture was then refluxed for 3 h. After leaving the solution for 2 days at room temperature, fine red colored crystals were isolated. Crystals of most complexes were suitable for single crystal X-ray analysis.

[MoO<sub>2</sub>L<sup>1</sup>(C<sub>2</sub>H<sub>5</sub>OH)](**1**): Yield: 0.29 g (60%). *Anal. Calc.* for C<sub>20</sub>H<sub>18</sub>N<sub>2</sub>O<sub>6</sub>Mo: C, 50.20; H, 3.76; N, 5.85. Found: C, 50.18; H, 3.77; N, 5.84%. <sup>1</sup>H NMR (DMSO-d<sub>6</sub>, 400 MHz) δ; 11.41 (s, 1H, aryl-OH), 10.07 (s, 1H, HC=N), 8.61–6.99 (m, 10H, Aromatic), 4.36 (s, 1H, OH-ethanol), 3.42 (q, 2H, CH<sub>2</sub>-ethanol), 1.05 (s, 3H, CH<sub>3</sub>-ethanol) ppm. <sup>13</sup>C NMR (DMSO-d<sub>6</sub>, 100 MHz) δ; 168.19, 160.20, 158.59, 152.76, 136.14, 134.01, 132.51, 129.03, 128.99, 128.89, 128.49, 124.91, 121.87, 120.25, 119.38, 117.10, 113.21, 111.65, 56.00, 18.54.

$[MoO_2L^2(CH_3OH)]$  (**2**): Yield: 0.23 g (53%). *Anal. Calc.* for  $C_{19}H_{17}N_3O_5Mo$ : C, 49.24; H, 3.67; N, 9.07. Found: C, 49.25; H, 3.64; N, 9.08%.  $^1H$  NMR (DMSO- $d_6$ , 400 MHz)  $\delta$ : 9.92 (s, 1H, HC=N), 8.57–6.62 (m, 10H, Aromatic), 7.12 (s, 2H,  $NH_2$ ), 4.10 (s, 1H, OH-methanol), 3.15 (s, 3H,  $CH_3$ -methanol) ppm.  $^{13}C$  NMR (DMSO- $d_6$ , 100 MHz)  $\delta$ : 169.06, 160.58, 151.88, 150.05, 135.93, 133.56, 132.91, 130.33, 129.44, 129.25, 128.77, 125.15, 122.16, 120.86, 116.51, 115.18, 112.26, 109.63, 49.07.

$[MoO_2L^3]$  (**3**): Yield: 0.26 g (54%). *Anal. Calc.* for  $C_{19}H_{14}N_2O_4Mo$ : C, 66.97; H, 3.25; N, 6.51. Found: C, 66.95; H, 3.26; N, 6.50%.  $^1H$  NMR (DMSO- $d_6$ , 400 MHz)  $\delta$ : 8.11–7.18 (m, 11H, Aromatic), 2.93 (s, 3H,  $CH_3$ ), ppm.  $^{13}C$  NMR (DMSO- $d_6$ , 100 MHz)  $\delta$ : 169.36, 165.06, 163.01, 152.34, 134.25, 132.43, 131.88, 130.98, 130.13, 129.24, 128.52, 127.84, 126.07, 125.02, 120.38, 119.84, 116.46, 113.69, 24.23.

$[MoO_2L^4]$  (**4**): Yield: 0.21 g (52%). *Anal. Calc.* for  $C_{19}H_{15}N_3O_4Mo$ : C, 51.23; H, 3.37; N, 9.43. Found: C, 51.24; H, 3.35; N, 9.44%.  $^1H$  NMR (DMSO- $d_6$ , 400 MHz)  $\delta$ : 8.01–6.87 (m, 10H, Aromatic), 7.04 (s, 2H,  $NH_2$ ), 2.86 (s, 3H,  $CH_3$ ) ppm.  $^{13}C$  NMR (DMSO- $d_6$ , 100 MHz)  $\delta$ : 170.36, 162.91, 162.82, 150.17, 134.03, 133.14, 131.87, 130.36, 130.07, 129.37, 127.77, 126.08, 124.96, 120.38, 119.82, 116.53, 115.47, 110.15, 24.40.

## 2.5. Synthesis of mixed-ligand complex $[MoO_2L^1(Q)]$ , where $Q = \gamma$ -picoline (**1a**)

To a clear red solution of **1** (0.50 mmol) in  $CH_3CN$  (30 mL),  $\gamma$ -picoline (0.73 mmol) was added and the reaction mixture was refluxed for 3 h. Slow evaporation of the red filtrate over 2 days produced dark red crystals. These were separated by filtration. Yield 0.25 g (57%). *Anal. Calc.* for  $C_{24}H_{19}N_3O_5Mo$ : C, 54.85; H, 3.61; N, 8.00. Found: C, 54.86; H, 3.59; N, 8.01%.  $^1H$  NMR (DMSO- $d_6$ , 400 MHz)  $\delta$ : 11.42 (s, 1H, aryl-OH), 10.08 (s, 1H, HC=N), 8.62–6.99 (m, 10H, Aromatic), 7.24–6.97 (m, 4H, Aromatic- $\gamma$ -picoline), 2.31 (s, 3H,  $CH_3$ - $\gamma$ -picoline) ppm.  $^{13}C$  NMR (DMSO- $d_6$ , 100 MHz)  $\delta$ : 168.69, 160.70, 159.09, 149.76, 147.22, 136.62, 134.49, 133.00, 129.52, 129.52, 129.47, 129.38, 128.97, 125.38,

125.11, 122.35, 120.73, 119.85, 117.58, 113.71, 112.15, 56.50, 20.88, 19.02.

## 2.6. Crystallography

Suitable single crystal of **1**, **1a** and **2–4** was chosen for X-ray diffraction studies. Crystallographic data and details of refinement are given in Table 1. The unit cell parameters and the intensity data for the complexes (**1**, **2**, **3** and **4**) were collected at  $\sim 293$  K, on a Bruker Smart Apex CCD diffractometer and complex (**1a**) was collected at 100 K, on a Bruker Smart Apex II CCD diffractometer using graphite monochromated Mo  $K\alpha$  radiation ( $\lambda = 0.71073$  Å), employing the  $\omega$ - $2\theta$  scan techniques. The intensity data were corrected for Lorentz, polarization and absorption effects. The structures were solved using the SHELXS97 [47] and refined using the SHELXL97 [48] computer programs. The non-hydrogen atoms were refined anisotropically.

## 2.7. Catalytic reactions

### 2.7.1. Oxidation of benzoin

In a typical oxidation reaction, benzoin (1.06 g, 5 mmol), aqueous 30%  $H_2O_2$  (1.71 g, 15 mmol) and catalyst (0.0005 g) were mixed in methanol (10 mL). The reaction mixture was heated under reflux with stirring for 4 h. The progress of the reaction was monitored by withdrawing samples at different time intervals and samples were extracted with *n*-hexane and then analyzed quantitatively by gas chromatography. The effect of various parameters such as amount of catalyst, amount of oxidant, and solvent were checked to optimize the conditions for the best performance of the catalyst. The identity of the products was confirmed by GC-mass.

### 2.7.2. Oxidative bromination of salicylaldehyde

Salicylaldehyde (0.610 g, 5 mmol) was added to an aqueous solution (20 mL) of KBr (1.785 g, 15 mmol), followed by addition of aqueous 30%  $H_2O_2$  (1.71 g, 15 mmol) in a 100 mL reaction flask.

**Table 1**  
Crystal and refinement data of complexes **1**, **1a**, **2**, **3** and **4**.

Compound	<b>1</b>	<b>1a</b>	<b>2</b>	<b>3</b>	<b>4</b>
Formula	$C_{20}H_{18}N_2O_6Mo$	$C_{24}H_{19}N_3O_5Mo$	$C_{19}H_{17}N_3O_5Mo$	$C_{19}H_{14}N_2O_4Mo$	$C_{19}H_{15}N_3O_4Mo$
M	478.30	525.36	463.30	430.26	445.28
Crystal symmetry	triclinic	monoclinic	triclinic	monoclinic	monoclinic
Space group	$P\bar{1}$	$P2_1/c$	$P\bar{1}$	$P2_1/c$	$P2_1/n$
<i>a</i> (Å)	7.8196(2)	13.313(2)	8.1198(5)	4.0623(12)	7.8923(3)
<i>b</i> (Å)	11.1222(3)	8.0476(14)	9.9276(6)	25.842(8)	13.8894(5)
<i>c</i> (Å)	11.4265(3)	21.357(3)	12.3349(8)	15.761(5)	15.3314(6)
$\alpha$ (°)	80.0650(10)	90	101.8430(10)	90	90
$\beta$ (°)	85.1030(10)	111.844(11)	103.7180(10)	98.332(16)	100.355(2)
$\gamma$ (°)	82.1190(10)	90	91.6650(10)	90	90
<i>V</i> (Å <sup>3</sup> )	967.69(4)	2123.9(6)	942.23(10)	1637.1(9)	1653.24(11)
Z	2	4	2	4	4
<i>D</i> <sub>calc</sub> (g cm <sup>-3</sup> )	1.642	1.643	1.633	1.746	1.789
<i>F</i> (000)	484	1064	468	864	896
$\mu$ (Mo $K\alpha$ ) (mm <sup>-1</sup> )	0.718	0.661	0.732	0.830	0.827
Max./min. trans.	0.9514/0.8999	0.9934/0.9804	0.9370/0.8981	0.9755/0.9366	0.9918/0.9598
$2\theta$ (max) (°)	26.00	25.42	26.00	25.00	25.99
Reflections collected/unique	15934/3799	61361/3914	9689/3671	25568/2871	26992/3249
$R_1^a [I > 2\sigma(I)]$	$R_1 = 0.0274$ , $wR_2 = 0.0685$	$R_1 = 0.0746$ , $wR_2 = 0.1208$	$R_1 = 0.0249$ , $wR_2 = 0.0668$	$R_1 = 0.0654$ , $wR_2 = 0.1639$	$R_1 = 0.0396$ , $wR_2 = 0.0943$
$wR_2^b$ [all data]	$R_1 = 0.0313$ , $wR_2 = 0.0715$	$R_1 = 0.1345$ , $wR_2 = 0.1390$	$R_1 = 0.0267$ , $wR_2 = 0.0680$	$R_1 = 0.0740$ , $wR_2 = 0.1688$	$R_1 = 0.0641$ , $wR_2 = 0.1059$
S [Goodness of fit]	1.038	1.086	1.095	1.174	1.089
Min./max. res.(e.Å <sup>-3</sup> )	0.680/−0.427	1.225/−0.732	0.341/−0.229	1.855/−1.795	0.530/−0.567

<sup>a</sup>  $R_1 = \sum |F_o| - |F_c| / \sum |F_o|$ .

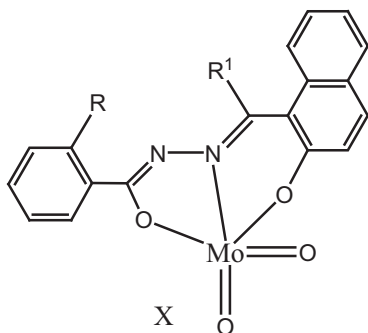
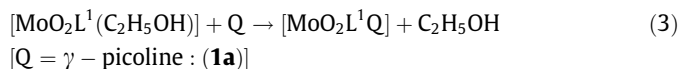
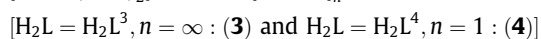
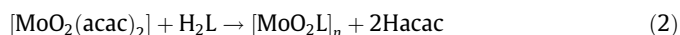
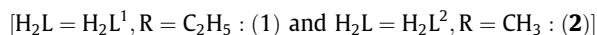
<sup>b</sup>  $wR_2 = \{ \sum [w(F_o^2 - F_c^2)]^2 / \sum [w(F_o^2)]^2 \}^{1/2}$ .

The catalyst (0.0005 g) and 70% HClO<sub>4</sub> (0.715 g, 5 mmol) were added, and the reaction mixture was stirred at room temperature (20 °C). Three additional 5 mmol portions of 70% HClO<sub>4</sub> were further added to the reaction mixture in three equal portions at 45 min intervals under continuous stirring. After 3 h, the separated white products were extracted with CH<sub>2</sub>Cl<sub>2</sub> and dried. The crude mass was dissolved in methanol and was subjected to gas chromatography. The identity of the products was confirmed as mentioned above.

### 3. Results and discussion

#### 3.1. Synthesis and spectral properties

Reactions of the selected aroylhydrazones (*c.f.* Scheme 1) with [MoO<sub>2</sub>(acac)<sub>2</sub>] in refluxing alcohol afforded two different types of Mo<sup>VI</sup> complexes, [MoO<sub>2</sub>L(ROH)] and [MoO<sub>2</sub>L]; Equations 1 and 2. The formation of mixed-ligand mononuclear complex [MoO<sub>2</sub>L(Q)] {where Q =  $\gamma$ -picoline (**1a**)} has been achieved by the reaction of **1** with  $\gamma$ -picoline; Equation 3. Proposed structures of these complexes (Scheme 2) are based on their spectroscopic characterization (IR, electronic and <sup>1</sup>H NMR spectroscopy), elemental analyses and single crystal X-ray diffraction studies. The ligands coordinate through their dianionic (ONO)<sup>2-</sup> enolate tautomeric forms.



Ligand	X	Complex
H <sub>2</sub> L <sup>1</sup>	C <sub>2</sub> H <sub>5</sub> OH	[MoO <sub>2</sub> L <sup>1</sup> (C <sub>2</sub> H <sub>5</sub> OH)] ( <b>1</b> )
H <sub>2</sub> L <sup>1</sup>	$\gamma$ -picoline	[MoO <sub>2</sub> L <sup>1</sup> ( $\gamma$ -pic)] ( <b>1a</b> )
H <sub>2</sub> L <sup>2</sup>	CH <sub>3</sub> OH	[MoO <sub>2</sub> L <sup>2</sup> (CH <sub>3</sub> OH)] ( <b>2</b> )
H <sub>2</sub> L <sup>3</sup>	--	[MoO <sub>2</sub> L <sup>3</sup> ] ( <b>3</b> )
H <sub>2</sub> L <sup>4</sup>	--	[MoO <sub>2</sub> L <sup>4</sup> ] ( <b>4</b> )

Scheme 2. Possible bonding modes of Mo(VI) complexes.

All these complexes are highly soluble in aprotic solvents, viz. DMF or DMSO and are sparingly soluble in alcohol, CH<sub>3</sub>CN and CHCl<sub>3</sub>. All these complexes are diamagnetic, indicating the presence of molybdenum in the +6 oxidation state, and are non-conducting in solution.

Spectral characteristics of compounds are listed in Table 2. The DMSO solutions of all the complexes display a medium intensity band in the 468–423 nm region (Fig. S1) and two strong absorptions in the 340–256 nm range, which are assignable to ligand to molybdenum ( $p\pi-d\pi$ ) charge transfer (LMCT) and intraligand transitions, respectively [16,49,50].

IR spectra of the complexes contain all the pertinent bands of the coordinated tridentate ligands [16,49,50]. In addition, **1**, **1a**, **2** and **4** display two strong peaks in the range 937–902 cm<sup>-1</sup> due to terminal  $\nu(\text{M}=\text{O}_t)$  stretching [16,49–51]. There are two relatively strong and broad peaks around 821–863 cm<sup>-1</sup> due to weakened (Mo–O → Mo) for oligomeric complex **3**, observed. The details of IR spectra of the free ligands and their corresponding dioxidomolybdenum (VI) complexes are given in Table 2.

The <sup>1</sup>H and <sup>13</sup>C NMR (DMSO-d<sub>6</sub>) data of all the free ligands and their corresponding dioxidomolybdenum(VI) complexes are given in the experimental section. The spectra of the free ligands exhibit a resonance at  $\delta = 12.97$ – $10.31$  due to naphthyl –OH (H<sub>2</sub>L<sup>1–4</sup>), at  $\delta = 9.54$ – $9.47$  due to –HC=N protons (H<sub>2</sub>L<sup>1–2</sup>) and at  $\delta = 2.35$ – $2.34$  due to –CH<sub>3</sub> protons (H<sub>2</sub>L<sup>3–4</sup>), respectively. All the aromatic protons of ligands are clearly observed in the expected region  $\delta = 8.33$ – $6.23$ . In the NMR spectra of complexes, the absence of signal due to aromatic (naphthyl) –OH indicates that the phenolic group is coordinated to the metal centre after proton replacement [16,49,50]. Similarly, the absence of signal due to –NH proton in the complexes suggests that the ligands are coordinated to the metal center via enolic form.

#### 3.2. Electrochemical properties

Electrochemical properties of the complexes have been studied by cyclic voltammetry in DMF solution (0.1 M TBAP). Voltammetric data are given in Table 3. The CV traces of the complexes exhibit two irreversible reductive responses within the potential window –0.73 to –1.08 V, which are assigned to Mo<sup>VI</sup>/Mo<sup>V</sup> and Mo<sup>V</sup>/Mo<sup>IV</sup> processes respectively. The lack of anodic response, even at a higher scan rate, is clearly due to rapid decomposition of the reduced species [16,49,50].

#### 3.3. X-ray structure of complexes

Complexes **1** and **2** are isostructural *cis*-dioxidomolybdenum(VI) species; hence, details of **2** are not discussed here. Only complex **1** as a representative case is discussed here. Selected bond angles and bond lengths for both are given in Table 4 for comparison purposes. The molecular structure and the atom numbering scheme of complex **2** is shown in Fig. S2.

##### 3.3.1. Description of the X-ray structure of complex **1** and **3**

The molecular structure and the atom numbering scheme for the complex [MoO<sub>2</sub>L<sup>1</sup>(C<sub>2</sub>H<sub>5</sub>OH)] (**1**) and [MoO<sub>2</sub>L<sup>3</sup>] (**3**) are shown in Fig. 1 and Fig. S3 respectively; the relevant bond distances and angles are collected in Table 4. The coordination geometry around the molybdenum (VI) atom in **1** and **3** reveals a distorted octahedral environment with an NO<sub>5</sub> coordination sphere (Scheme 2). Each ligand molecule behaves as a dianionic tridentate one and bonded to the metal centre through the phenolate oxygen O(1), the enolate oxygen O(2) and the imine nitrogen N(1). In both the complexes, one of the two oxo group O(4) is located trans to the imine nitrogen in the same plane. For complex **1** the other oxo group O(3) is located in the axial plane with the solvent molecule,

**Table 2**Characteristic IR<sup>a</sup> bands ( $\nu$  in  $\text{cm}^{-1}$ ) and electronic spectral data<sup>b</sup> for the studied complexes (**1**, **1a** and **2–4**).

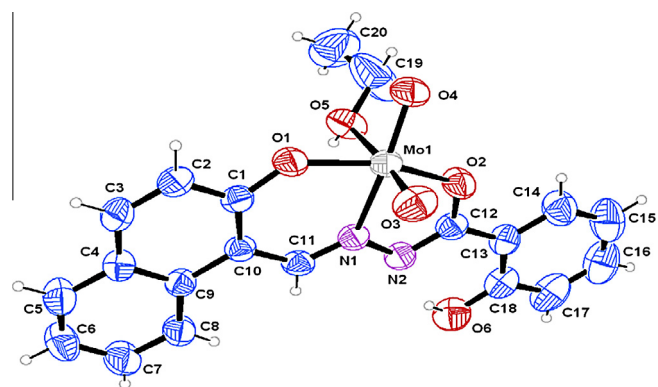
Complex	$\nu(\text{C}=\text{O})$	$\nu(\text{C}=\text{N})$	$\nu(\text{N}=\text{N})$	$\nu(\text{Mo}=\text{O})$	$\lambda_{\text{max}}$ (nm) ( $\epsilon/\text{dm}^3 \text{mol}^{-1} \text{cm}^{-1}$ )
H <sub>2</sub> L <sup>1</sup>	1621	1610	–	–	–
H <sub>2</sub> L <sup>2</sup>	1637	1602	–	–	–
H <sub>2</sub> L <sup>3</sup>	1652	1622	–	–	–
H <sub>2</sub> L <sup>4</sup>	1652	1619	–	–	–
[MoO <sub>2</sub> L <sup>1</sup> (C <sub>2</sub> H <sub>5</sub> OH)] ( <b>1</b> )	–	1602	1038	937, 913	447 (5890), 340 (1591), 257 (1915)
[MoO <sub>2</sub> L <sup>1</sup> ( $\gamma$ -pic)] ( <b>1a</b> )	–	1595	975	923, 902	446 (5505), 339 (1361), 257 (1770)
[MoO <sub>2</sub> L <sup>2</sup> (CH <sub>3</sub> OH)] ( <b>2</b> )	–	1597	1021	931, 902	468 (51649), 329 (12711), 256 (13024)
[MoO <sub>2</sub> L <sup>3</sup> ] ( <b>3</b> )	–	1594	1045	863, 821	423 (10701), 329 (23470), 258 (20373)
[MoO <sub>2</sub> L <sup>4</sup> ] ( <b>4</b> )	–	1590	1049	935, 908	442 (10433), 329 (14886), 258 (27667)

<sup>a</sup> In KBr pellet.<sup>b</sup> In DMSO.**Table 3**Cyclic voltammetric results for dioxidomolybdenum (VI) complexes (**1**, **1a** and **2–4**) at 298 K.

Complex	Epc [V] <sup>a</sup>
[MoO <sub>2</sub> L <sup>1</sup> (C <sub>2</sub> H <sub>5</sub> OH)] ( <b>1</b> )	–0.81, –1.03
[MoO <sub>2</sub> L <sup>1</sup> ( $\gamma$ -pic)] ( <b>1a</b> )	–0.79, –1.06
[MoO <sub>2</sub> L <sup>2</sup> (CH <sub>3</sub> OH)] ( <b>2</b> )	–0.73, –1.08
[MoO <sub>2</sub> L <sup>3</sup> ] ( <b>3</b> )	–0.75, –1.07
[MoO <sub>2</sub> L <sup>4</sup> ] ( <b>4</b> )	–0.77, –1.06

<sup>a</sup> Solvent: DMF; working electrode: platinum; auxiliary electrode: platinum; reference electrode: Ag/AgCl; supporting electrolyte: 0.1 M TBAP; scan rate: 50 mV/s. Epc is the cathodic peak potential.

C<sub>2</sub>H<sub>5</sub>OH. Whereas in complex **3** along with the two oxo-oxygen, O(3) and O(4), the three ONO donor points of the ligand complete the five coordinate environment around the Mo(VI) acceptor center, the disposition of the donor points being roughly square pyramidal. The sixth coordination site, trans to the oxo-oxygen O(3), is occupied by an oxo-oxygen O(3<sup>1</sup>) of the next neighboring complex molecule and this pattern is repeated leading to a chain of MoO<sub>2</sub>L<sup>3</sup> molecules (Fig. 2). This may be visualized as an effect of stacking of the complex molecules along the z-axis [52] The length of the Mo–O(3<sup>1</sup>) bond (2.374 (5) Å) is considerably longer

**Fig. 1.** ORTEP diagram of [MoO<sub>2</sub>L<sup>1</sup>(C<sub>2</sub>H<sub>5</sub>OH)], **1** with atom labeling scheme. Thermal ellipsoids have been drawn at 50% probability.

than the other Mo–O bonds, the longest of which [Mo–O(2)] is 1.980 (5) Å which suggests that this should be explained as oligomeric structure where one of the oxygen of one molybdenum weakly interacts with other. The bond between Mo and the azomethine nitrogen in the complexes are within the range of

**Table 4**Selected bond distances [Å] and bond angles [°] for Complexes **1**, **1a**, **2**, **3** and **4**.

	Complex <b>1</b>	Complex <b>1a</b>	Complex <b>2</b>	Complex <b>3</b>	Complex <b>4</b>
<i>Bond lengths</i>					
Mo(1)–O(1)	1.918(2)	1.917(5)	1.925(1)	1.894(5)	1.923(3)
Mo(1)–O(2)	2.000(2)	2.017(5)	1.992(1)	1.980(5)	1.991(3)
Mo(1)–O(3)	1.694(2)	1.697(4)	1.693(2)	1.702(5)	1.690(3)
Mo(1)–O(4)	1.698(2)	1.713(4)	1.706(2)	1.687(5)	1.701(3)
Mo(1)–O(5)	2.385(2)	–	2.297(2)	–	–
Mo(1)–N(1)	2.225(2)	2.222(4)	2.234(2)	2.233(5)	2.222(3)
Mo(1)–N(3)	–	2.429(5)	–	–	–
Mo(1)–O(3)#1	–	–	–	2.374(5)	–
<i>Bond angles</i>					
O(1)–Mo(1)–O(2)	149.48(8)	148.8(2)	146.77(6)	146.8(2)	147.0(1)
O(1)–Mo(1)–O(3)	99.77(9)	101.2(2)	99.23(8)	101.0(2)	99.8(1)
O(1)–Mo(1)–O(4)	102.67(9)	101.8(2)	104.27(7)	100.8(2)	101.8(1)
O(1)–Mo(1)–O(5)	80.25(7)	–	79.32(6)	–	–
O(1)–Mo(1)–N(1)	80.55(7)	80.0(2)	80.11(6)	79.2(2)	80.3(1)
O(2)–Mo(1)–O(3)	97.25(9)	95.8(2)	99.39(7)	99.3(2)	100.9(1)
O(2)–Mo(1)–O(4)	96.70(9)	98.5(2)	97.06(7)	98.6(2)	96.3(1)
O(2)–Mo(1)–O(5)	79.46(7)	–	78.16(6)	–	–
O(2)–Mo(1)–N(1)	72.33(8)	72.5(2)	71.88(6)	72.4(2)	72.2(1)
O(3)–Mo(1)–O(4)	105.9(1)	105.4(2)	105.20(8)	105.7(3)	107.1(1)
O(3)–Mo(1)–O(5)	172.03(9)	–	171.37(8)	–	–
O(3)–Mo(1)–N(1)	97.07(9)	95.4(2)	92.26(7)	97.5(2)	96.3(1)
O(4)–Mo(1)–O(5)	81.75(8)	–	83.37(7)	–	–
O(4)–Mo(1)–N(1)	155.70(9)	158.2(2)	160.84(7)	156.2(2)	155.6(1)
O(5)–Mo(1)–N(1)	75.03(7)	–	79.10(6)	–	–
O(3)–Mo(1)–O(3)#1	–	–	–	170.8(2)	–

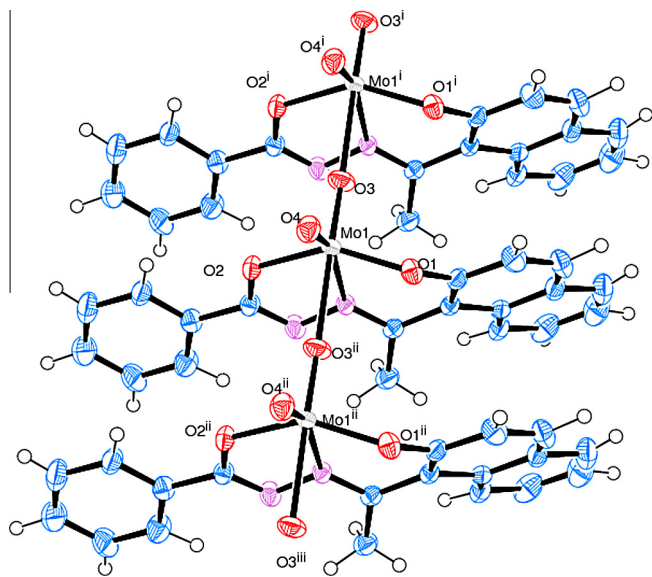


Fig. 2. One dimensional polymeric diagram of  $[\text{MoO}_2\text{L}^3]$ , **3**. Thermal ellipsoids have been drawn at 50% probability.

2.225–2.233 Å, which is comparatively longer than other Mo–N single bonds. This is due to the trans effect generated by the oxo group trans to the Mo–N bond [49]. The angular distortion in the octahedral environment around Mo comes from the bites taken by the Schiff base ligand, angles O(1)–Mo(1)–N(1) is 80.55 (7)° and 79.2 (2)° and angles O(2)–Mo(1)–N(1) is 72.33(8)° and 72.4 (2)° for complexes **1** and **3** respectively. For the same reason the *trans* angles O(1)–Mo(1)–O(2) and O(4)–Mo(1)–N(1) are significantly reduced from the ideal value of 180°. The *trans*-axial angle O(3)–Mo(1)–O(5) for complex **1** is 172.03(9)°.

### 3.3.2. Description of the X-ray structure of complex 1a

The atom numbering scheme of complex **1a** is given in Fig. 3 with the relevant bond distances and angles collected in Table 4. The molecular structure of complex,  $[\text{MoO}_2\text{L}^1(\gamma\text{-pic})]$  has shown that the dinegative hydrazone ligand ( $\text{H}_2\text{L}^1$ ) binds to the molybdenum(VI) center by O(1), N(1) and O(2)- donor atoms. The fourth

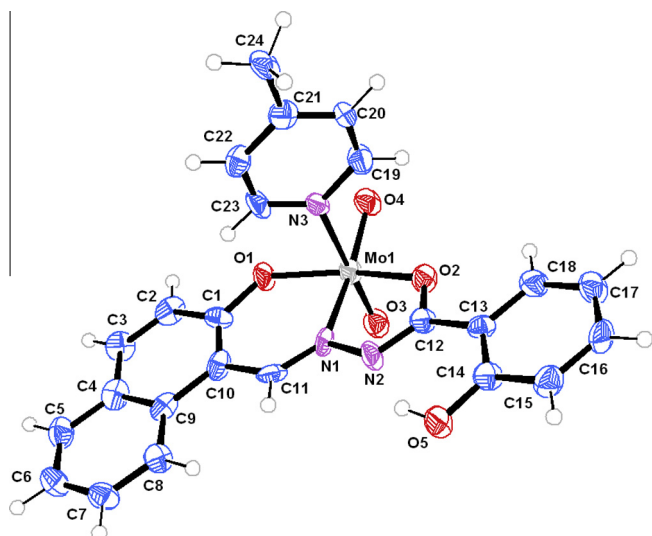


Fig. 3. ORTEP diagram of  $[\text{MoO}_2\text{L}^1(\gamma\text{-pic})]$ , **1a** with atom labeling scheme. Thermal ellipsoids have been drawn at 50% probability.

coordination site around molybdenum(VI) is occupied by a  $\gamma$ -picoline ligand in complex **1a** through its tertiary nitrogen N (3), forming a distorted octahedral complex. The rather large Mo(1)–N(3) distance [2.429 (5) Å] revealed that the  $\gamma$ -picoline moiety is also rather weakly coordinated to the  $\text{MoO}_2^{2+}$  core [16,19,50]. The Mo–O (oxo) bond distances of the  $\text{MoO}_2^{2+}$  group is unexceptional [16,19,50] and almost equal [1.697 (4)–1.713 (4) Å]. The ligand coordinates to the  $\text{MoO}_2^{2+}$  core in the deprotonated enolate form because in complexes **1** and **1a** the C–O bond distances [C(12)–O(2)] exhibit values of 1.316 (3) and 1.322 (7) Å respectively and are closer to a C–O single bond than to a C–O double bond distance. However, it falls short of the pure C–O single bond distance of 1.42 Å because of the delocalization of electrons.

### 3.3.3. Description of the X-ray structure of complex 4

We have employed the steric bulk on aroylhydrazones ligand ( $\text{H}_2\text{L}^4$ ) (Scheme 1) to gain control of the coordination number around the Mo(VI) center. Structural studies indicate that, with increasing steric bulk, control of the coordination number around the Mo(VI) center is achieved by the formation of 5-coordinate dioxidomolybdenum(VI) complex of the type  $[\text{MoO}_2\text{L}^4]$  (**4**) (Scheme 2). The molecular structure and the atom numbering scheme of **4** is shown in Fig. 4. In this compound ( $\text{MoO}_2\text{L}^4$ ) the coordination geometry of Mo(VI) is similar to that observed earlier [50], which consist of two oxo oxygen atoms, one enolate oxygen, one phenolate oxygen, and an azomethine nitrogen atom. This is the rare example of a five-coordinate Mo(VI) complex [50,53]. No structural evidence for the achievement of hexacoordination through Mo–O...Mo bridging is observed. The molecular geometry of  $\text{MoO}_2\text{L}^4$  is best represented as a square-pyramid with one axial oxo oxygen atom [O(3)], and three O atoms [O(1,2,4)] and the N(1) atom describing the equatorial plane, which is slightly distorted from an ideal geometry, as reflected in the bond parameters (Table 4) around the metal center. The length of the Mo–O(4) bond lying *trans* to N(1) is practically equal to Mo–O(3); the position *trans* to O(3) remains unoccupied. The other Mo–O and Mo–N distances are normal, as observed in other structurally characterized complexes of molybdenum containing these bonds [49,50]. The bite angles of the ligand at molybdenum, O(2)–Mo(1)–N(1) and O(1)–Mo(1)–N(1) are 72.2 (1)° and 80.3 (1)°, respectively, generating five-membered and six-membered chelate rings at the Mo<sup>VI</sup> center.

## 3.4. Catalytic activity studies

### 3.4.1. Oxidation of benzoin

The oxidation of benzoin has attracted the attention of researchers because one of its oxidized products, benzil, is a very useful intermediate for the synthesis of heterocyclic compounds

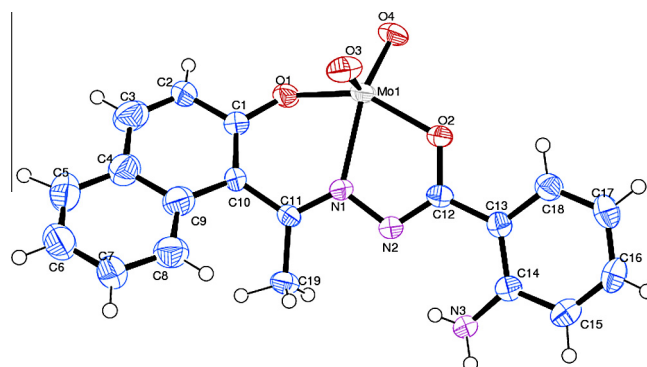


Fig. 4. ORTEP diagram of  $[\text{MoO}_2\text{L}^4]$ , **4** with atom labeling scheme. Thermal ellipsoids have been drawn at 50% probability.

and benzylic acid rearrangements [54]. The oxidation of benzoin was successfully achieved with the molybdenum complexes using 30% aqueous  $\text{H}_2\text{O}_2$  as oxidant. The products mainly obtained were benzoic acid, benzaldehyde-dimethylacetal, methylbenzoate and benzil (Scheme 3).

To optimize the reaction conditions for the maximum oxidation of benzoin,  $[\text{MoO}_2\text{L}^2(\text{CH}_3\text{OH})]$  (**2**) was considered as a representative catalyst. The effect of oxidant was studied by considering the substrate to oxidant ratios of 1:1, 1:2 and 1:3 for the fixed amount of catalyst (0.0005 g) and substrate (1.06 g, 5 mmol) in 10 mL of refluxing methanol. As shown in Fig. 5 and entry No. 3 of Table 5, a maximum of 96% conversion of benzoin was achieved at the substrate to oxidant ratio of 1: 3, in 4 h of reaction time. Lowering the amount of oxidant decreases the conversion. The effect of amount of catalyst on the oxidation of benzoin was studied considering three different amounts of  $[\text{MoO}_2\text{L}^2(\text{CH}_3\text{OH})]$  (**2**) viz. 0.0005, 0.001 and 0.0015 g for the fixed amount of benzoin (1.06 g, 5 mmol) and 30%  $\text{H}_2\text{O}_2$  (1.7 g, 15 mmol) in 10 mL of methanol and the reaction was monitored at reflux temperature of methanol. A maximum of 96% conversion was achieved with 0.0005 g of catalyst. This conversion improved only marginally to 98% whereas 0.0015 g of catalyst gave a maximum conversion of 99% in 4 h of reaction time (Fig. 6). Thus at the expense of catalyst, only 0.0005 g of catalyst can be considered sufficient to optimize other reaction conditions. The amount of solvent also influences the oxidation of benzoin. It was concluded (Fig. 7 and entry No. 3, 4 and 5 of Table 5) that 10 mL methanol was sufficient to effect maximum conversion under above optimized reaction conditions. Table 6 summarizes conversion of benzoin under different experimental conditions. Thus, from these experiments, the best reaction conditions for the maximum oxidation of benzoin as concluded are: catalyst  $[\text{MoO}_2\text{L}^2(\text{CH}_3\text{OH})]$  (**2**) (0.0005 g), benzoin (1.06 g, 5 mmol), 30%  $\text{H}_2\text{O}_2$  (1.7 g, 15 mmol) and refluxing methanol (10 mL).

Fig. 8 presents the selectivity of products along with the conversion of benzoin as a function of time (4 h) under the optimal experimental conditions as concluded above, i.e. benzoin (1.06 g, 5 mmol), 30%  $\text{H}_2\text{O}_2$  (1.7 g, 15 mmol),  $[\text{MoO}_2\text{L}^2(\text{CH}_3\text{OH})]$  (**2**) (0.0005 g), and methanol (10 mL) under reflux condition. It is clear from the plot that all products form with the conversion of benzoin. The highest selectivity of benzoic acid (ca. 51%) was observed in the first one hour. With the elapse of time its selectivity slowly decreases and finally becomes almost constant and reaches 47% after 4 h. Similar results have been observed in case of methyl benzoate and benzil and reach 23% and 16%, respectively. The selectivity of benzaldehyde-dimethylacetal increases continuously from 3% to 14%. Thus, with the maximum benzoin oxidation of 96% after 4 h of reaction time, the selectivity of the reaction products varies in the order: benzoic acid (47%) > methyl benzoate (23%), > benzil (16%) > benzaldehyde-dimethylacetal (14%).

Under these reaction conditions other catalysts were also tested and results are compared in Fig. 9 while Table 6 provides turnover frequency (TOF) and selectivity details. The data presented in the table show that other complexes are also catalytically active and show equally good activity with very high turnover frequency (TOF: 1021–1301  $\text{h}^{-1}$ ) but the selectivity order of various products

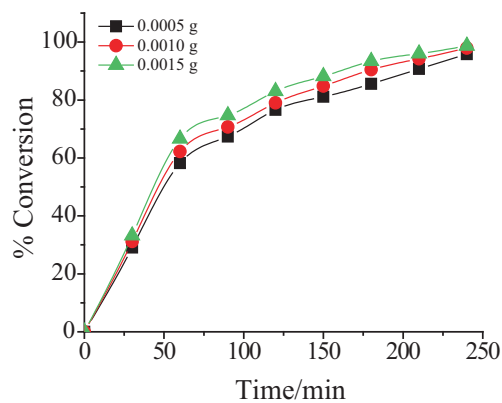


Fig. 5. Effect of catalyst amount on the oxidation of benzoin. Reaction conditions: benzoin (1.06 g, 5 mmol), 30%  $\text{H}_2\text{O}_2$  (1.7 g, 15 mmol) and methanol (10 mL).

Table 5

Conversion of benzoin (1.06 g, 5 mmol) using  $[\text{MoO}_2\text{L}^2(\text{CH}_3\text{OH})]$  (**2**) as catalyst in 4 h of reaction time under different reaction conditions.

Entry No.	Catalyst (g)	$\text{H}_2\text{O}_2$ (g mmol)	$\text{CH}_3\text{OH}$ (ml)	Conversion (%)
1	0.0005	0.57, 05	10	83
2	0.0005	1.14, 10	10	88
3	0.0005	1.71, 15	10	96
4	0.0005	1.71, 15	15	89
5	0.0005	1.71, 15	20	81
6	0.001	1.71, 15	10	98
7	0.0015	1.71, 15	10	99

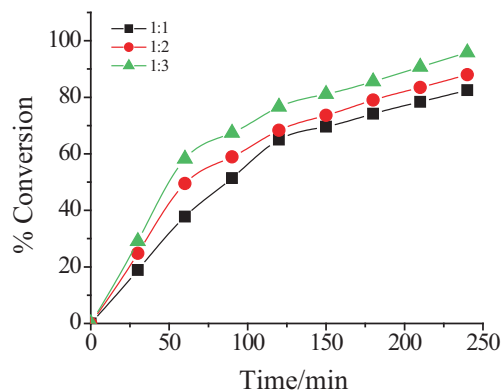
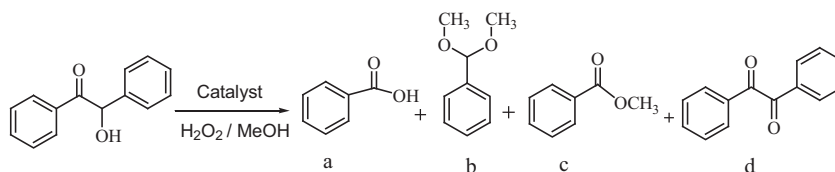
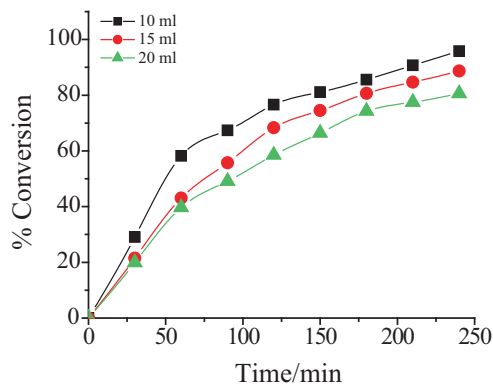


Fig. 6. Effect of oxidant amount on the oxidation of benzoin. Reaction conditions: benzoin (1.06 g, 5 mmol), catalyst amount (0.0005 g) and methanol (10 mL).

slightly differs. In the absence of the catalyst, the reaction mixture showed 60% conversion where selectivity of different products follows the order: benzil (48%) > benzoic acid (27%) > benzaldehyde-dimethylacetal (20%) > methyl benzoate (5%). Thus, these



Scheme 3. Various oxidation products of benzoin. (a) benzoic acid, (b) benzaldehyde-dimethylacetal, (c) methylbenzoate and (d) benzil.



**Fig. 7.** Effect of solvent (methanol) amount on the oxidation of benzoin. Reaction conditions: benzoin (1.06 g, 5 mmol), catalyst amount (0.0005 g) and 30% H<sub>2</sub>O<sub>2</sub> (1.7 g, 15 mmol).

**Table 6**  
Effect of different catalysts on the oxidation of benzoin, TOF and product selectivity.

Catalyst (g)	TOF (h <sup>-1</sup> )	Conversion (%)	Selectivity (%) <sup>a</sup>			
			a	b	c	D
[MoO <sub>2</sub> L <sup>1</sup> (C <sub>2</sub> H <sub>5</sub> OH)] (1)	1148	96	29	22	31	18
[MoO <sub>2</sub> L <sup>1</sup> ( $\gamma$ -pic)] (1a)	1301	99	31	26	26	17
[MoO <sub>2</sub> L <sup>2</sup> (CH <sub>3</sub> OH)] (2)	1110	96	47	14	23	16
[MoO <sub>2</sub> L <sup>3</sup> ] (3)	1021	95	40	25	22	13
[MoO <sub>2</sub> L <sup>4</sup> ] (4)	1073	96	40	24	22	14
Without catalyst		60	27	20	5	48

<sup>a</sup> (a) Benzoic acid, (b) benzaldehyde-dimethylacetal, (c) methylbenzoate and (d) benzil.

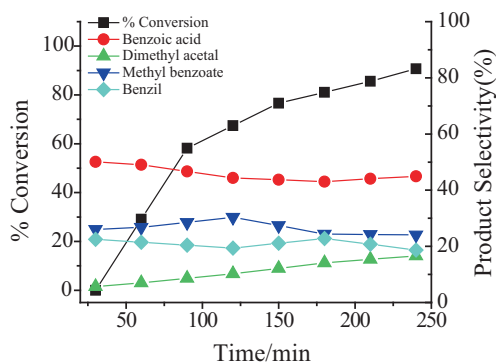


**Fig. 8.** Plot showing percentage conversion of benzoin and the selectivity of benzoic acid, benzaldehyde dimethylacetal, methyl benzoate and benzil formation as a function of time. Reaction condition: benzoin (1.06 g, 5 mmol), H<sub>2</sub>O<sub>2</sub> (1.7 g, 15 mmol), [MoO<sub>2</sub>L<sup>2</sup>(CH<sub>3</sub>OH)] (2) (0.0005 g) and 10 mL methanol.

complexes not only enhance the catalytic action, they also alter the selectivity of the products.

#### 3.4.2. Oxidative bromination of salicylaldehyde

Oxidative bromination of salicylaldehyde, a functional mimic of haloperoxidases, in aqueous solution at room temperature has also been carried out successfully. By using these dioxidomolybdenum(VI) complexes as catalyst precursors in the presence of KBr, HClO<sub>4</sub> and H<sub>2</sub>O<sub>2</sub> gave mainly three products, namely 5-bromosalicylaldehyde, 3,5-dibromosalicylaldehyde and 2,4,6-tribromophenol; (Scheme 4). After several trials (Table 7), the best suited reaction conditions obtained for the maximum conversion of 5 mmol (0.610 g) of salicylaldehyde were: KBr (1.785 g, 15 mmol), aqueous 30% H<sub>2</sub>O<sub>2</sub> (1.71 g, 15 mmol), catalyst (0.0005), aqueous

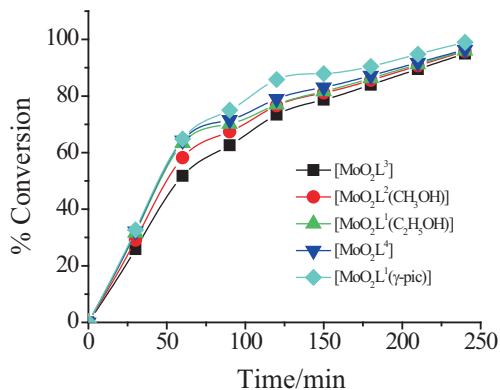


**Fig. 9.** Comparison of various catalysts on the oxidation of benzoin. Reaction conditions: benzoin (1.06 g, 5 mmol), 30% H<sub>2</sub>O<sub>2</sub> (1.7 gm, 15 mmol), catalyst amount (0.0005 gm) and methanol (10 mL).

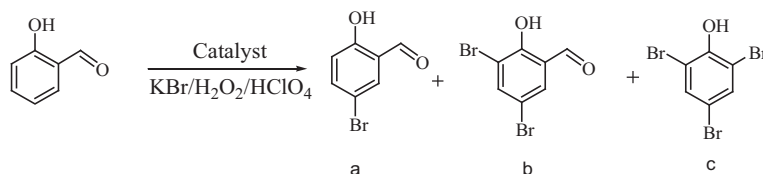
70% HClO<sub>4</sub> (2.86 g, 20 mmol) and water (20 mL). However, the addition of HClO<sub>4</sub> in four equal portions (at  $t=0, 45, 90$  and 135 min. of reaction time) was necessary to improve the conversion of the substrate and to avoid decomposition of the catalyst. A total of 3 h was required to complete the reaction. Under the above conditions, a maximum of 96% conversion was achieved with [MoO<sub>2</sub>L<sup>2</sup>(CH<sub>3</sub>OH)] (2) and all three products were identified; Table 7. The presence of three equivalent of H<sub>2</sub>O<sub>2</sub> facilitates not only the formation of HOBr, which ultimately helps in the oxidative bromination of salicylaldehyde but also affects on the selectivity of different products. Other catalysts gave similar results. Lowering the amount of H<sub>2</sub>O<sub>2</sub> increased the formation of 5-bromosalicylaldehyde. In the absence of the catalyst, the reaction mixture gave ca. 40% conversion of salicylaldehyde where selectivity of the formation of 5-bromosalicylaldehyde is 89%.

Other complexes have also been tested under similar reaction conditions and the results obtained are summarized in Table 8. It is clear from the table that all the complexes have equally good catalytic potential with high turnover frequency. The selectivity of the 5-bromosalicylaldehyde (56.5–75%) is much high for most complexes except for [MoO<sub>2</sub>L<sup>4</sup>] (4) which exhibits only 47.5% selectivity. The overall selectivity of three products follows the order: 5-bromosalicylaldehyde > 2,4,6-tribromophenol > 3,5-dibromosalicylaldehyde.

A noteworthy feature of the present catalytic reactions is that, the recovered solutions of catalysts from the catalytic reaction mixture were found active up to two cycles with nearly same conversion (Table S1 and S2). The selectivity of reaction products of benzoin was also found nearly same but in case of salicylaldehyde, the catalyst became more selective towards 5-bromosalicylaldehyde with no formation of tribromo derivative.

#### 3.4.3. Reactivity of complexes with H<sub>2</sub>O<sub>2</sub>

Dioxidomolybdenum (VI) complexes are known to react with H<sub>2</sub>O<sub>2</sub> to form the corresponding oxidoperoxo complexes. In order to throw some light on the reaction mechanism of catalytic reactions, complex [MoO<sub>2</sub>L<sup>2</sup>(CH<sub>3</sub>OH)] (2) dissolved in DMSO was reacted with H<sub>2</sub>O<sub>2</sub> and spectral changes were monitored by electronic absorption spectroscopy. Thus, the stepwise additions of H<sub>2</sub>O<sub>2</sub> (1.47 g, 13 mmol of 30% H<sub>2</sub>O<sub>2</sub> dissolved in 5 mL of DMSO) to 25 mL of ca.  $6.7 \times 10^{-3}$  M solution of [MoO<sub>2</sub>L<sup>2</sup>(CH<sub>3</sub>OH)] (2) in DMSO causes the decrease in the intensities of the 468 nm band and finally disappear (Fig. 10). Simultaneously, two bands start appearing at 369 and 383 nm and become intense after addition of excess of H<sub>2</sub>O<sub>2</sub>. The intensity of the 337 nm band decreases slowly along with the appearance of a shoulder band at ca.



**Scheme 4.** Main products obtained upon oxidative bromination of salicylaldehyde. (a) 5-bromosalicylaldehyde, (b) 3,5-dibromosalicylaldehyde and (c) 2,4,6-tribromophenol.

**Table 7**

Results of oxidative bromination of salicylaldehyde catalyzed by  $[\text{MoO}_2\text{L}^2(\text{CH}_3\text{OH})]$  (**2**) after 3 h of contact time.

Entry No.	Catalyst (g)	$\text{H}_2\text{O}_2$ (g mmol)	KBr (g mmol)	$\text{HClO}_4$ (g mmol)	Conversion (%)
1	0.0005	0.57, 5	1.78, 15	2.86, 20	66
2	0.0005	1.14, 10	1.78, 15	2.86, 20	81
3	0.0005	1.71, 15	1.78, 15	2.86, 20	96
4	0.0005	1.71, 15	0.59, 5	2.86, 20	57
5	0.0005	1.71, 15	1.19, 10	2.86, 20	77
6	0.0005	1.71, 15	1.78, 15	1.43, 10	67
7	0.0005	1.71, 15	1.78, 15	2.14, 15	89
8	0.0010	1.71, 15	1.78, 15	2.86, 20	98
9	0.0015	1.71, 15	1.78, 15	2.86, 20	99

**Table 8**

Effect of different catalysts on the oxidative bromination of salicylaldehyde, TOF and product selectivity.

Catalyst (g)	TOF ( $\text{h}^{-1}$ )	Conversion (%)	Selectivity (%) <sup>a</sup>		
			Monobromo	Dibromo	Tribromo
$[\text{MoO}_2\text{L}^1(\text{C}_2\text{H}_5\text{OH})]$ ( <b>1</b> )	1555	98	60.6	1.6	37.8
$[\text{MoO}_2\text{L}^1(\gamma\text{-pic})]$ ( <b>1a</b> )	1673	95	75	4.4	20.5
$[\text{MoO}_2\text{L}^2(\text{CH}_3\text{OH})]$ ( <b>2</b> )	1482	96	75	12.1	12.6
$[\text{MoO}_2\text{L}^3]$ ( <b>3</b> )	1415	99	56.6	1.7	41.7
$[\text{MoO}_2\text{L}^4]$ ( <b>4</b> )	1470	99	47.5	1.6	51.0
Without catalyst		40	89	0.2	10.8

<sup>a</sup> (a) 5-Bromosalicylaldehyde, (b) 3,5-dibromosalicylaldehyde and (c) 2,4,6-tribromophenol.

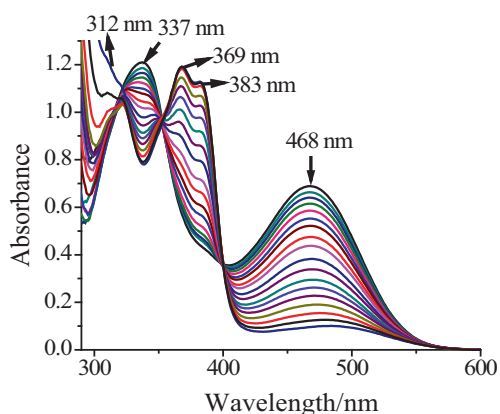


**Fig. 10.** UV-Vis spectral changes observed during titration of  $[\text{MoO}_2\text{L}^2(\text{CH}_3\text{OH})]$ , **2** with  $\text{H}_2\text{O}_2$ . The spectra were recorded after successive additions of 1-drop portions of 30%  $\text{H}_2\text{O}_2$  (13 mmol) dissolved in 5 mL of DMSO to 25 mL of  $6.7 \times 10^{-3}$  M solution in DMSO.

320 nm. We have interpreted this result in terms of the formation of the oxidoperoxidomolybdenum(VI) complex. The new bands at 383 and 368 nm may be assigned to LMCT and  $n-\pi^*$  transitions, respectively. The latter one was not visible in  $[\text{MoO}_2\text{L}^2(\text{CH}_3\text{OH})]$  (**2**) while the band at 320 nm is assignable to  $\pi-\pi^*$  transition. The oxidoperoxidomolybdenum(VI) complex finally transfers oxygen to the benzoin to give the various oxidation products. The intermediate peroxido complex is likely to form hydroperoxidomolybdenum(VI) complex also in the presence of  $\text{H}^+$  that oxidizes

a bromide ion to give bromine equivalent intermediate(s). Such an intermediate may then brominate an appropriate organic substrate [55].

#### 4. Conclusions

Synthesis of four new dioxidomolybdenum(VI) complexes with aroylhydrazone of naphthol-derivative (**1**, **2**, **3** and **4**) and one mixed-ligand mononuclear complex (**1a**) have been prepared and characterized. The one labile binding site in these complexes has an added advantage as has been shown by reacting complex **2** with  $\text{H}_2\text{O}_2$  to give corresponding peroxido species without changing original coordinating sites i.e. ONO coordination of ligands. Again the labile peroxido group of complexes has an added advantage as they transfer oxygen in catalytic oxidation as has been demonstrated for the oxidation by peroxide, of benzoin using these complexes as catalysts. Under optimized reaction conditions benzoin gives 95–99% conversion with four reaction products benzoic acid, benzaldehyde–dimethylacetal, methylbenzoate and benzil. The functional mimic of haloperoxidase is demonstrated by the oxidative bromination of salicylaldehyde where these complexes have shown 95–99% conversion of salicylaldehyde to brominated and other products with high turnover frequency.

#### Declaration

I do also hereby declare that the work described in the submission is new and has not been published previously. It is not under

consideration for publication elsewhere. Its publication is approved by all authors and explicitly by the responsible authorities where the work was carried out.

### Acknowledgements

The authors thank the reviewers for their comments and suggestions, which were helpful in preparing the revised version of the manuscript. We acknowledge the use of UV–Vis spectrophotometer purchased from a DST (India) Grant No. SR/FT/CS-016/2008. S. Pasayat and Y. P. Patil gratefully acknowledge the Council of Scientific and Industrial Research, New Delhi, India, for the award of research fellowship.

### Appendix A. Supplementary data

CCDC 831865, 924877, 831864, 885367 and 885366 contains the supplementary crystallographic data for **1**, **1a**, **2**, **3** and **4**. These data can be obtained free of charge via <http://www.ccdc.cam.ac.uk/conts/retrieving.html>, or from the Cambridge Crystallographic Data Centre, 12 Union Road, Cambridge CB2 1EZ, UK; fax: +44 1223 336 033; or e-mail: [deposit@ccdc.cam.ac.uk](mailto:deposit@ccdc.cam.ac.uk). Supplementary data associated with this article can be found, in the online version, at <http://dx.doi.org/10.1016/j.poly.2013.08.055>.

### References

- [1] A.A.A. Abu-Hussen, J. Coord. Chem. 59 (2006) 157.
- [2] M.S. Karthikeyan, D.J. Prasad, B. Poojary, K.S. Bhat, Bioorg. Med. Chem. 14 (2006) 7482.
- [3] K. Singh, M.S. Barwa, P. Tyagi, Eur. J. Med. Chem. 41 (2006) 147.
- [4] P. Pannerselvam, R.R. Nair, G. Vijayalakshmi, E.H. Subramanian, S.K. Sridhar, Eur. J. Med. Chem. 40 (2005) 225.
- [5] S.K. Sridhar, M. Saravanan, A. Ramesh, Eur. J. Med. Chem. 36 (2001) 615.
- [6] S.N. Pandeya, D. Sriram, G. Nath, E. De Clercq, Eur. J. Pharm. Sci. 9 (1999) 25.
- [7] R. Mladenova, M. Ignatova, N. Manolova, T.S. Petrova, I. Rashkov, Eur. Polym. J. 38 (2002) 989.
- [8] O.M. Walsh, M.J. Meegan, R.M. Prendergast, T.A. Nakib, Eur. J. Med. Chem. 31 (1996) 989.
- [9] Z. Trávníček, M. Maloň, Z. Šindelář, K. Doležal, J. Rolčík, V. Kryštof, M. Strnad, J. Marek, J. Inorg. Biochem. 84 (2001) 23.
- [10] U. El-Ayaan, A.A.M. Abdel-Aziz, Eur. J. Med. Chem. 40 (2005) 1214.
- [11] M. Sönmez, I. Berber, E. Akbaş, Eur. J. Med. Chem. 41 (2006) 101.
- [12] M.R. Maurya, S. Agarwal, M. Abid, A. Azam, C. Bader, M. Ebel, D. Rehder, Dalton Trans. (2006) 937.
- [13] D.K. Johnson, T.B. Murphy, N.J. Rose, W.H. Goodwin, L. Pickart, Inorg. Chim. Acta 67 (1982) 159.
- [14] T.B. Chaston, D.B. Lovejoy, R.N. Watts, D.R. Richardson, Clin. Cancer Res. 9 (2003) 402.
- [15] G. Link, P. Ponka, A.M. Konijn, W. Breuer, Z.I. Cabantchik, C. Hershko, Blood 101 (2003) 4172.
- [16] S. Pasayat, S.P. Dash, Saswati, P.K. Majhi, Y.P. Patil, M. Nethaji, H.R. Dash, S. Das, R. Dinda, Polyhedron 38 (2012) 198.
- [17] S.P. Dash, S. Pasayat, Saswati, H.R. Dash, S. Das, R.J. Butcher, R. Dinda, Polyhedron 31 (2012) 524.
- [18] R. Dinda, P.K. Majhi, P. Sengupta, S. Pasayat, S. Ghosh, L.R. Falvello, T.C.W. Mak, Polyhedron 29 (2010) 248.
- [19] J.H. Enemark, J.J.A. Cooney, J.J. Wang, R.H. Holm, Chem. Rev. 104 (2004) 1175.
- [20] E.I. Stiefel, Met. Ions Biol. Syst. 39 (2002) 727.
- [21] R. Hille, Chem. Rev. 96 (1996) 2757.
- [22] D. Collison, C.D. Garner, J.A. Joule, Chem. Soc. Rev. 25 (1996) 25.
- [23] J.T. Hoffman, S. Einwaechter, B.S. Chohan, P. Basu, C.J. Carrano, Inorg. Chem. 43 (2004) 7573.
- [24] A. Sigel, H. Sigel (Eds.), Metal Ions in Biological Systems 39, Molybdenum and Tungsten, Their Roles in Biological Processes, Marcel Dekker, New York, 2002.
- [25] R.C. Bray, B. Adams, A.T. Smith, B. Bennett, S. Bailey, Biochemistry 39 (2000) 11258.
- [26] K. Jeyakumar, D.K. Chand, J. Chem. Sci. 121 (2009) 111.
- [27] M.R. Maurya, Curr. Org. Chem. 16 (2012) 73.
- [28] R.D. Chakravarthy, K. Suresh, V. Ramkumar, D.K. Chand, Inorg. Chim. Acta 376 (2011) 57.
- [29] Z. Hu, X. Fu, Y. Li, Inorg. Chem. Commun. 14 (2011) 497.
- [30] M. Herbert, F. Montilla, A. Galindo, J. Mol. Catal. A: Chem. 338 (2011) 111.
- [31] A. Rezaeifard, I. Sheikhsheoie, N. Monadi, M. Alipour, Polyhedron 29 (2010) 2703.
- [32] I. Sheikhsheoie, A. Rezaeifard, N. Monadi, S. Kaafi, Polyhedron 28 (2009) 733.
- [33] A. Gunyara, D. Betzb, M. Dreesb, E. Herdtweck, F.E. Kuhna, J. Mol. Catal. A: Chem. 331 (2010) 117.
- [34] M.R. Maurya, S. Sikarwar, P. Manikandan, Appl. Catal. A 315 (2006) 74.
- [35] A.J. Burke, Coord. Chem. Rev. 252 (2008) 170.
- [36] K.R. Jain, W.A. Herrmann, F.E. Kuhn, Coord. Chem. Rev. 252 (2008) 556.
- [37] K.C. Gupta, A.K. Sutar, Coord. Chem. Rev. 252 (2008) 1420.
- [38] B. Frédéric, Coord. Chem. Rev. 236 (2003) 71.
- [39] A. Syamal, M.R. Maurya, Coord. Chem. Rev. 95 (1989) 183.
- [40] R.A. Sheldon, J.K. Kochi, Metal Catalyzed Oxidations of Organic Compounds, Academic Press, New York, 1981.
- [41] B.M. Trost, I. Fleming, S.V. Ley (Eds.), Comprehensive Organic Synthesis, Pergamon, Oxford, 7 (1991) 251.
- [42] G.J.-J. Chen, J.W. McDonald, W.E. Newton, Inorg. Chem. 15 (1976) 2612.
- [43] I. Kizilcikli, S. Eğlence, A. Gelir, B. Ülküseven, Transition Met. Chem. 33 (2008) 775.
- [44] A. Syamal, D. Kumar, Transition Met. Chem. 7 (1982) 118.
- [45] A. Syamal, D. Kumar, J. Ind. Chem. Soc. 65 (1988) 112.
- [46] R.L. Dutta, A.K. Pal, Ind. J. Chem. A. 22 (1983) 871.
- [47] G.M. Sheldrick, SHELXS-97, Program for Crystal Structure Determination, Universität Göttingen, Göttingen, Germany, 1997.
- [48] G.M. Sheldrick, SHELXL-97, Program for Refinement of Crystal Structures, Universität Göttingen, Göttingen, Germany, 1997.
- [49] R. Dinda, P. Sengupta, S. Ghosh, H.M. Figge, W.S. Sheldrick, Dalton Trans. (2002) 4434.
- [50] R. Dinda, P. Sengupta, S. Ghosh, W.S. Sheldrick, Eur. J. Inorg. Chem. (2003) 363.
- [51] R.D.R.S. Manian, R. Leino, O. Wichmann, A. Lehtonen, Inorg. Chem. Commun. 12 (2009) 1004.
- [52] N.R. Pramanik, S. Ghosh, T.K. Raychaudhuri, S. Ray, R.J. Butcher, S.S. Mandal, Polyhedron 23 (2004) 1595.
- [53] T.A. Hanna, A.K. Ghosh, C. Ibarra, M.A. Mendez-Rojas, A.L. Rheingold, W.H. Watson, Inorg. Chem. 43 (2004) 1511.
- [54] G.B. Gill, in: G. Pattenden (Ed.), Comprehensive Organic Synthesis, vol. 3, Pergamon Press, New York, 1991, p. 821.
- [55] A. Butler, M.J. Clague, G.E. Meister, Chem. Rev. 94 (1994) 625.